RRM2-mediated Wnt/β-catenin signaling pathway activation in lung adenocarcinoma: A potential prognostic biomarker

YONGJIE JIANG*, XING HU*, MIN PANG, YUYAN HUANG, BI REN, LIPING HE and LI JIANG

Department of Respiratory and Critical Care Medicine, The Affiliated Hospital of North Sichuan Medical College, Nanchong, Sichuan 637000, P.R. China

Received April 6, 2023; Accepted July 17, 2023

DOI: 10.3892/ol.2023.14003

Abstract. The present study aimed to investigate the role and mechanism of action of ribonucleotide reductase M2 (RRM2) in lung adenocarcinoma and its potential as a therapeutic target. Data of patients with lung adenocarcinoma from The Cancer Genome Atlas database were collected and analyzed to evaluate the potential of RRM2 as a biomarker. The expression of RRM2 was evaluated in the A549 cell line and its cisplatin-resistant A549/DDP cell line derivative by western blot and reverse transcription-quantitative PCR. The study also investigated cell proliferation and the mechanism by which RRM2 controls cellular cisplatin resistance using CCK-8 and colony-formation assays. In addition, cell migration was assessed using Transwell assays, and the cell cycle and apoptosis were examined using flow cytometry. RRM2 was highly expressed in lung adenocarcinoma and was associated with the clinical TMN stage. Functional enrichment analysis showed that RRM2 was enriched in the cell cycle. Immune cell infiltration analysis identified 12 types of immune cell that exhibited differences between patients expressing different levels of RRM2. Cellular assays revealed higher levels of RRM2 expression in A549/DDP cells than A549 cells, and its expression was induced by cisplatin. RRM2 knockdown decreased cell proliferation and migration, accelerated apoptosis and caused cell cycle arrest in the S-phase, increasing the sensitivity of A549 and A549/DDP cells to cisplatin through the Wnt/β-catenin signaling pathway. Overexpression of β-catenin reduced the effects of RRM2 knockdown on A549 cells. Lung adenocarcinoma growth may be influenced by RRM2 through the Wnt/β-catenin signaling pathway, suggesting a potential pathway for cancer progression.

Correspondence to: Professor Li Jiang, Department of Respiratory and Critical Care Medicine, The Affiliated Hospital of North Sichuan Medical College, 1 MaoYuan South Road, Shunqing, Nanchong, Sichuan 637000, P.R. China
E-mail: lanqilily@163.com

*Contributed equally

Key words: ribonucleotide reductase M2, lung adenocarcinoma, Wnt/β-catenin signaling pathway, cell cycle, apoptosis

Introduction

Lung cancer has the second highest incidence and the highest mortality rate among all cancers worldwide. Non-small cell lung cancer (NSCLC) is the most common type of lung cancer, accounting for ~80-85% of all lung cancers, and lung adenocarcinoma is a diverse form of NSCLC (1,2). While molecularly targeted drugs and immune-based therapies have recently been developed, chemotherapy remains the primary method of treatment for patients with advanced lung adenocarcinoma (3). Cisplatin, one of the most commonly used chemotherapeutic agents in clinical practice, often leads to chemotherapy failure due to inherent or acquired cisplatin resistance (4). Therefore, understanding how tumors grow and identifying the causes of tumor drug resistance is necessary to effectively treat lung adenocarcinoma.

Ribonucleotide reductases are a family of enzymes that perform vital biological functions by catalyzing the conversion of four common nucleotides into deoxy-ribonucleoside triphosphate (dNTP), which is required for DNA replication and repair (5). Ribonucleotide reductase M2 (RRM2) is a component of ribonucleotide reductase. It has been reported that tumor cells express RRM2 in the late G1 and early S phases of the cell cycle, and regulate DNA replication and repair by controlling the synthesis of dNTPs (6). RRM2 is an oncogene that is highly expressed in cancers such as hepatocellular carcinoma (7) and colorectal cancer (8,9). It is not only associated with cancer cell proliferation, migration, invasion and apoptosis, but it also has a role in the chemotherapy resistance of cancer cells. For instance, inhibition of RRM2 expression not only enhances the sensitivity of pancreatic cancer cells (10,11) and squamous cell carcinoma cells (12) to gemcitabine, but also enhances the sensitivity of ovarian cancer cells (13-15) to cisplatin. RRM2 may be used as a biomarker in NSCLC (16-18) to detect chemotherapy sensitivity and predict the prognosis of patients, and understanding the role of RRM2 in lung adenocarcinoma and how it works is critical to developing more effective treatments for this disease.

The Wnt signaling pathway is a complex regulatory network with three major components: Wnt/β-catenin, Wnt/planar cell polarity and Wnt/Ca^{2+}. The Wnt/β-catenin signaling

pathway transports accumulated cytoplasmic β-catenin to the nucleus and has a key role in embryonic development, stem cell self-renewal and tumorigenesis by activating downstream target genes (19,20). Previous studies have reported that RRM2 is overexpressed in hepatocellular carcinoma and promotes the proliferation and migration ability of hepatocellular carcinoma cells through the Wnt/β-catenin signaling pathway (21). RRM2 may also affect cell proliferation and apoptosis through the Wnt/β-catenin signaling pathway when overexpressed in multiple myeloma cells (22). However, research on RRM2 in lung adenocarcinoma is currently limited. Therefore, the present study used a bioinformatics analysis of lung adenocarcinoma data from The Cancer Genome Atlas (TCGA) database to investigate the role of RRM2 in lung adenocarcinoma proliferation, migration, apoptosis and cisplatin resistance formation using A549 and cisplatin-resistant A549 (A549/DDP) cells.

Materials and methods

Bioinformatics analysis. Lung adenocarcinoma data were obtained from the TCGA website (https://portal.gdc.cancer.gov/) and processed using Perl (v5.30.1) and the R software (v4.1.3). Gene expression analysis and clinical characterization were performed using the limma, ggplot2 and ggpubr packages. Survival analysis was performed with the survival and survminer packages. Receiver operating characteristic (ROC) curves were plotted using the TimeROC package. Kyoto Encyclopedia of Genes and Genomes (KEGG) pathway prediction and gene set enrichment analysis (GSEA) were performed with filter conditions set at |log2 fold change|>1 and false discovery rate <0.05. Differential analysis of the tumor microenvironment (TME) was performed using the estimate package and immune cell infiltration analysis was performed using the cibersort algorithm.

Cell culture and cell transfection. The lung adenocarcinoma cell lines A549 and A549/DDP were cultured in Ham's F-12K medium supplemented with 10% FBS (100 U/ml penicillin, 100 mg/l streptomycin) and incubated at 37˚C, 5% CO_2 and 95% humidity. A549/DDP cells were cultured with a final concentration of 1 μg/ml DDP. Cell lines and reagents were purchased from Pricella. RRM2 knockdown was performed using a lentiviral vector (shRRM2) obtained from GenePharma. The sense sequence of the vector is 5'-GATCCGTAGAGAGAACCCATTTGACTTTATTCAAGAGATAAAGTCAAATGGGGTTCTCTATTTTTTG-3', while the antisense sequence is 5'-AATTCAAAAAATAGAGAGAACCCATTTGACTTTATCTCTTGAATAAAGTCAAATGGGTTCTCTACG-3'. As for the negative control (NC), it possesses a sense sequence of 5'-GATCCGTTCTCCGAACGTGTCACGTTTCAAGAGAACGTGACACGTTCGGAGAACTTTTTTG-3' and an antisense sequence of 5'-AATTCAAAAAAGTTCTCCGAACGTGTCACGTTCTCTTGAAACGTGACACGTTCGGAGAACG-3'. Before lentiviral transfection, cells were seeded in 6-well plates and transfected with the virus upon reaching 60-70% confluence. After transfection, cells were selected in complete medium containing 4 μg/ml puromycin. Remaining cells after one week were considered to have stable knockdown of RRM2 and were cultured in complete medium with 2 μg/ml puromycin for long-term culture. The overexpression plasmid of β-catenin and its negative control pcDNA3.1 were from Hanbio (cat. no. KWC20221122CDNWH-PC01). Before plasmid transfection, cells were seeded in 6-well plates. When the cells reached 60-70% confluence, 4 μg of the overexpression plasmid or its control were transfected into corresponding cells using 10 μl LipoFiter 3.0 (Hanbio). After 8 h, the old medium of the cells was replaced with fresh medium.

Reverse transcription-quantitative PCR (RT-qPCR). Total RNA was extracted using the TRIzol (Aidlab Biotechnologies Co., Ltd) method, followed by RT using the RevertAid First Strand cDNA Synthesis Kit (Thermo Fisher Scientific, Inc.) according to the manufacturer's instructions, to generate complementary DNA. Real-time qPCR was performed using the MagicSYBR Mixture (CoWin Biotech) following the manufacturer's instructions. Real-time qPCR was conducted on a QuantStudio™ 6 Flex instrument (Thermo Fisher Scientific, Inc.) with the following thermocycling conditions: Initial denaturation at 95˚C for 30 sec; denaturation at 95˚C for 5 sec, annealing/extension at 60˚C for 30 sec, for a total of 40 cycles; and melting curve analysis at 95˚C for 15 sec, 60˚C for 1 min, 95˚C for 15 sec and 50˚C for 30 sec. The gene primer sequences used were as follows: GAPDH forward, 5'-GGAGCGAGATCCCTCCAAAAT-3' and reverse, 5'-GGCTGTTGTCATACTTCTCATGG-3'; RRM2 forward, 5'-AGTGGAAGGCATTTTCTTTTCC-3' and reverse, 5'- GCAAAATCACAGTGTAAACCCT-3'; β-catenin forward, 5'-GGCTCTTGTGCGTACTGTCCTTC-3' and reverse, 5'-GCTTCTTGGTGTCGGCTGGTC-3'. The $2^{-\Delta\Delta Cq}$ formula (23) is used to calculate the relative expression levels of the target gene.

Western blot analysis. Each group of cells was lysed and denatured using Cell Lysis Buffer for Western and IP (Beyotime Institute of Biotechnology), and protein quantification was performed by the BCA method. A total of 25 μg of protein sample per lane was denatured and electrophoresed using 10% SDS-PAGE, followed by semi-dry transfer of protein onto a PVDF membrane (Immobilion-P; EMD Millipore) and protein blocking with Protein Free Rapid Blocking Buffer (Epizyme) at room temperature for 30 min. The membrane was then incubated with the following primary antibodies at 4˚C for 15 h: GAPDH (1:2,000 dilution; cat. no. AF1186; Beyotime Institute of Biotechnology), β-actin (1:2,000 dilution; cat. no. AF1186; Beyotime Institute of Biotechnology), RRM2 (1:1,000 dilution; cat. no. 11661-1-AP; Proteintech), β-catenin (1:1,000 dilution; cat. no. AC106; Beyotime Institute of Biotechnology), cyclin D1 (1:2,000 dilution; cat. no. AF0126; Beyotime Institute of Biotechnology) and c-MYC (1:2,000 dilution; cat. no. 10828-1-AP; Proteintech). Subsequently, it was incubated with HRP-labeled Goat Anti-Rabbit IgG (1:1,000 dilution; cat. no. A0208; Beyotime Institute of Biotechnology) for 1 h at room temperature and final visualization was performed using a GelDoc XR System (Bio-Rad Laboratories, Inc.). The experimental results were analyzed in grayscale using Image J (v1.8.0; National Institutes of Health).

CCK-8 assay. Cells were harvested and cultured in 96-well plates (Corning, Inc.) at a density of $3x10^3$ cells per 100 μl of medium, with five replicate wells per group. Upon cell

adhesion, the time was set to 0 h. Subsequently, cells were incubated in a constant temperature chamber at 37˚C and the medium was replaced with complete medium supplemented with 10 μl CCK-8 (Abbkine) per 100 μl at 0, 24, 48 or 72 h. After 1 h, the optical density (OD) at 450 nm was measured using a Varioskan LUX Multimode Reader (Thermo Fisher Scientific, Inc.).

Colony-formation assay. The experimental cells were harvested and seeded in a 6-well plate (Corning, Inc.) at a density of 600 cells per 2 ml of culture medium. A medium change was performed on the 6th day. On the 12th day, the 6-well plate was analyzed as follows: Cells were washed twice with PBS, fixed with 4% paraformaldehyde for 15 min, washed twice with PBS, stained with crystal 1% violet for 15 min and washed twice with PBS before analysis; all steps were conducted at room temperature. The wells were photographed using an optical microscope and colonies were manually counted. In this study, clusters of cells containing >50 cells were considered colonies.

Chemotherapy sensitivity assay. Experimental cells were harvested and seeded onto a 96-well plate at a density of $5x10^3$ cells per 100 μl of medium. For each group, six different concentrations of cisplatin were prepared and five wells were used for each concentration. After overnight cell culture, the medium was replaced with complete medium containing 0, 1, 2, 4, 8 and 16 μg/ml concentrations of cisplatin for the transfected A549 cells, and with 0, 4, 8, 16, 32 and 64 μg/ml concentrations of cisplatin for the transfected A549/DDP cells, followed by continuous cultivation for 24 h. The old medium was discarded and replaced with 100 μl complete medium containing 10 μl of CCK-8 (Abbkine). Following incubation at 37˚C for 2 h, the OD at 450 nm was measured using a Varioskan LUX Multimode Reader (Thermo Fisher Scientific, Inc.). The cell inhibition rate (%) was calculated as follows: (OD of control group-OD of experimental group)/(OD of control group-OD of blank group) x100%.

Transwell assays. Experiments were performed using 24-well plates (Corning, Inc.) and 8-μm pore size Transwell cell culture chambers (Falcon; Corning Life Science). Cells were collected by preparing a suspension of $5x10^4$ cells in 200 μl serum-free medium, which was added to the upper chamber. The lower chamber was filled with 600 μl complete medium containing 10% FBS. After 24 h of incubation, the Transwell chambers were removed and washed twice with PBS. The cells were then fixed with 4% paraformaldehyde for 15 min, washed twice with PBS, stained with 1% crystal violet for 15 min and washed twice with PBS. Fixing, washing and staining steps were conducted at room temperature. The cells in the upper chamber were removed with cotton swabs and three randomly selected fields of view were counted using an inverted fluorescence microscope (Leica Microsystems GmbH) at x400 magnification.

Cell cycle analysis and apoptosis assay. For cell cycle experiments, the experimental cells were seeded in 6-well plates at a density of $3x10^5$ cells per well, and were collected after 48 h of incubation. The cells were washed once with PBS and then fixed with 70% ethanol at 4˚C for 12 h. Following fixation, the cells were stained using the Cell Cycle and Apoptosis Analysis Kit (Beyotime Institute of Biotechnology) according to the manufacturer's instructions. Initially, 500 μl of staining buffer was added, followed by the addition of 25 μl propidium iodide staining solution and 10 μl RNase A. The cells were then incubated for 30 min at room temperature while being protected from light, and then analyzed using a flow cytometer.

For the apoptosis experiments, cells were seeded in 6-well plates at a density of $3x10^5$ cells per well and incubated for 24 h. The old medium was then removed and replaced with complete medium containing or lacking 2 μg/ml DDP for A549 cells, and complete medium containing or lacking 8 μg/ml DDP for A549/DDP cells. After 24 h of incubation, the cells were collected. Staining was performed using the Annexin V-APC/7-AAD Apoptosis Detection Kit (KeyGEN Biotech) according to the manufacturer's instructions. First, 500 μl of Binding Buffer was added, followed by 5 μl AnnexinV-APC and 5 μl 7-AAD, which were mixed thoroughly while avoiding light. The cells were then incubated for 10 min and analyzed using a flow cytometer.

Confocal microscopy. Complete medium (1 ml) containing $1.5x10^5$ cells was added to the BeyoGold™ 35 mm Confocal Dishes (Beyotime Institute of Biotechnology) and cells were allowed to attach by culture for 24 h. Following this, the medium in the confocal dish was replaced with complete medium containing 0 or 2 μg/ml cisplatin and incubation was continued for another 24 h. Subsequently, the cells were fixed with 4% paraformaldehyde for 15 min, Immunol Staining Blocking Buffer (Beyotime Institute of Biotechnology) was applied for 60 min, incubation with RRM2 primary antibody (cat. no. 11661-1-AP; 1:500 dilution; Proteintech) was performed for 1 h at room temperature and incubation with a fluorescent-labeled secondary antibody (cat. no. A0468; 1:500 dilution; Beyotime Institute of Biotechnology) for 1 h. All experiments were conducted at room temperature. Finally, fluorescence images were captured using a confocal microscope (FV3000; Olympus Corporation) after adding Antifade Mounting Medium with DAPI (Beyotime Institute of Biotechnology).

Statistical analysis. GraphPad Prism 9.0.0 (GraphPad Software; Dotmatics) was used for graphic representation of the data. The measurement data were expressed as the mean ± standard deviation. Statistical analysis was performed using SPSS 25.0 (IBM Corporation). The unpaired Student's t-test was used for comparisons between two groups, and one-way analysis of variance (ANOVA) followed by the Least Significant Difference (LSD) post-hoc test was used for comparisons between more than two groups. $P<0.05$ was considered to indicate a statistically significant difference.

Results

RRM2 is highly expressed in lung adenocarcinoma and is associated with patient prognosis and clinical features. By analyzing data from the TCGA database, it was found that RRM2 expression was elevated in lung adenocarcinoma compared to normal lung samples (Fig. 1A). Furthermore,

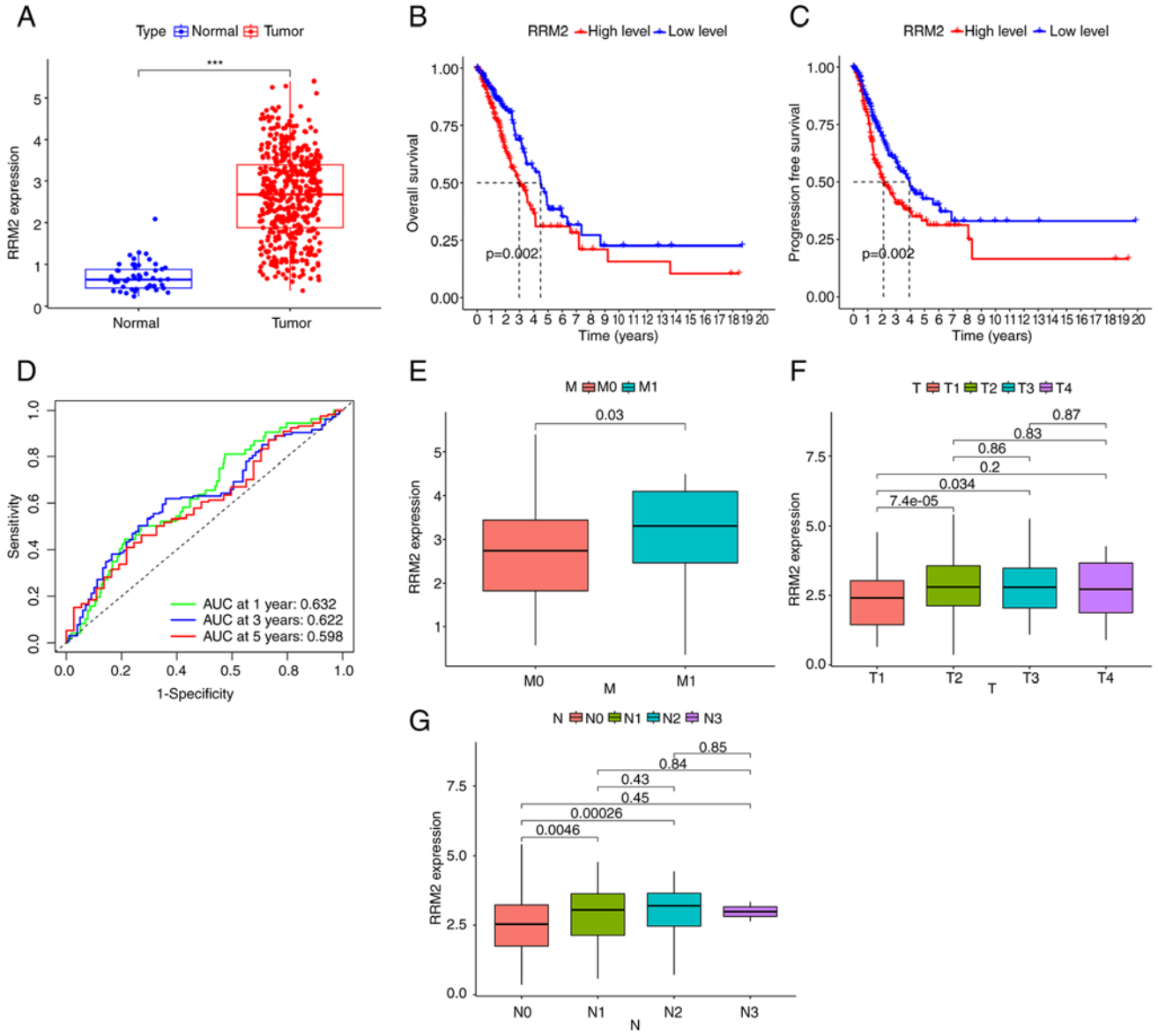

Figure 1. Bioinformatics analysis of the significance of RRM2 in lung adenocarcinoma. (A) Assessment of RRM2 expression levels in cancerous and paraneoplastic tissues of lung adenocarcinoma. Evaluation of (B) overall survival and (C) progression-free survival of patients with lung adenocarcinoma expressing different levels of RRM2. (D) ROC curves predicting 1-, 3- and 5-year survival of patients based on RRM2 expression levels. (E-G) Analysis of the relationship between RRM2 expression levels and clinical characteristics. (E) Metastasis, (F) tumor and (N) nodal stage. ***P<0.001. RRM2, ribonucleotide reductase M2; ROC, receiver operating characteristic; AUC, area under the ROC curve.

patients with low RRM2 expression had longer overall and progression-free survival than those with high RRM2 expression (Fig. 1B and C). Using RRM2 to predict patient survival, the area under the curve was 0.632, 0.622 and 0.598 for 1, 2 and 5 years, respectively (Fig. 1D). In the TNM classification of lung adenocarcinoma, stage M1 with distant metastasis exhibited higher RRM2 expression levels than stage M0 without metastasis (Fig. 1E). In addition, stages T2 and T3, which represent larger tumor sizes, showed elevated RRM2 expression compared to stage T1 (Fig. 1F). Similarly, stages N1 and N2, involving lymph node metastasis, displayed higher RRM2 expression levels than stage N0 without lymph node involvement (Fig. 1G). However, no statistically significant difference was observed in RRM2 expression levels between patients at T4 and T1, and N3 and N1 stages, possibly due to the limited number of patients at stages T4 and N3 in the database.

Results of enrichment analysis and immune infiltration analysis. The KEGG enrichment analysis and GSEA revealed that genes associated with RRM2 were significantly enriched in the cell cycle in tumor samples, particularly in lung adenocarcinoma tissues with high RRM2 expression (Fig. 2A and B). Furthermore, analysis of the TME indicated significant differences in the StromalScore and ESTIMATEScore between patients with high and low RRM2 expression, but no difference in the ImmuneScore (Fig. 2C). The results of the immune cell differential and correlation analysis in the tumor tissues of patients with lung adenocarcinoma indicated that there were differences in the levels of 12 immune cells, namely B cells naive, T cells CD8, T cells CD4 memory resting, T cells CD4 memory activated, natural killer (NK) cells resting, NK cells activated, monocytes, macrophages M0, macrophages M1, dendritic cells resting, dendritic cells activated and mast

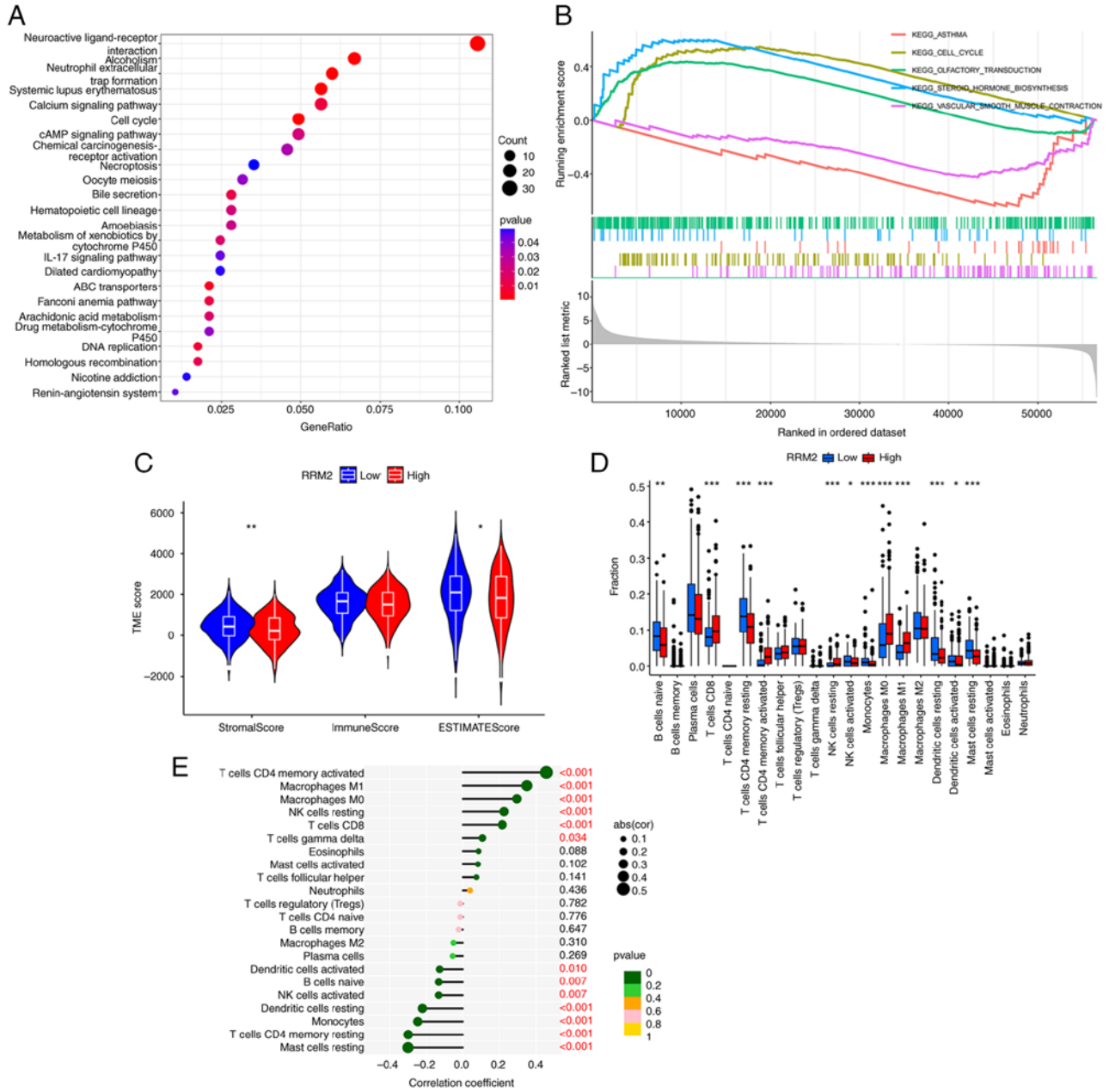

Figure 2. Results of enrichment analysis and immune infiltration analysis (A) KEGG pathway analysis and (B) gene set enrichment analysis results. (C) Comparison of the TME in patients with lung adenocarcinoma expressing different levels of RRM2. (D) Differential analysis and (E) correlation analysis of immune cells in lung adenocarcinoma tissues expressing different levels of RRM2. *P<0.05, **P<0.01, ***P<0.001. RRM2, ribonucleotide reductase M2; KEGG, Kyoto Encyclopedia of Genes and Genomes; NK, natural killer; TME, tumor microenvironment; abs, absolute value.

cells resting, between patients expressing different levels of RRM2. In addition, the expression levels of T cells CD4 memory activated, macrophages M1, macrophages M0, NK cells resting, T cells CD8 and T cells gamma delta were positively associated with RRM2 expression, while dendritic cells activated, B cells naive, NK cells activated, dendritic cells resting, monocytes, T cells CD4 memory resting and mast cells resting were negatively correlated with RRM2 expression levels (Fig. 2D and E).

RRM2 is highly expressed in cisplatin-resistant lung adenocarcinoma cells and cisplatin induces RRM2 expression in lung adenocarcinoma cells. RT-qPCR and western blot analyses demonstrated that RRM2 expression was significantly upregulated in cisplatin-resistant A549/DDP cells compared to A549 cells (Fig. 3A and B). Subsequently, A549 cells were treated with cisplatin concentrations of 0, 0.5, 1.5, and 2 μg/ml for 48 h, while A549/DDP cells were treated with cisplatin concentrations of 0, 1, 1.5 and 2 μg/ml for the same period. The results suggested that cisplatin treatment led to a decrease in RRM2 mRNA expression levels in A549 cells (Fig. 3C). However, a gradual increase in RRM2 mRNA expression was observed with higher concentrations of cisplatin (Fig. 3C). In contrast to the mRNA expression levels, the protein expression of RRM2 in A549 cells did not decrease upon cisplatin treatment but showed a progressive increase throughout the experiment (Fig. 3E). In A549/DDP cells, both RT-qPCR and western blot analysis revealed an increase in RRM2 expression

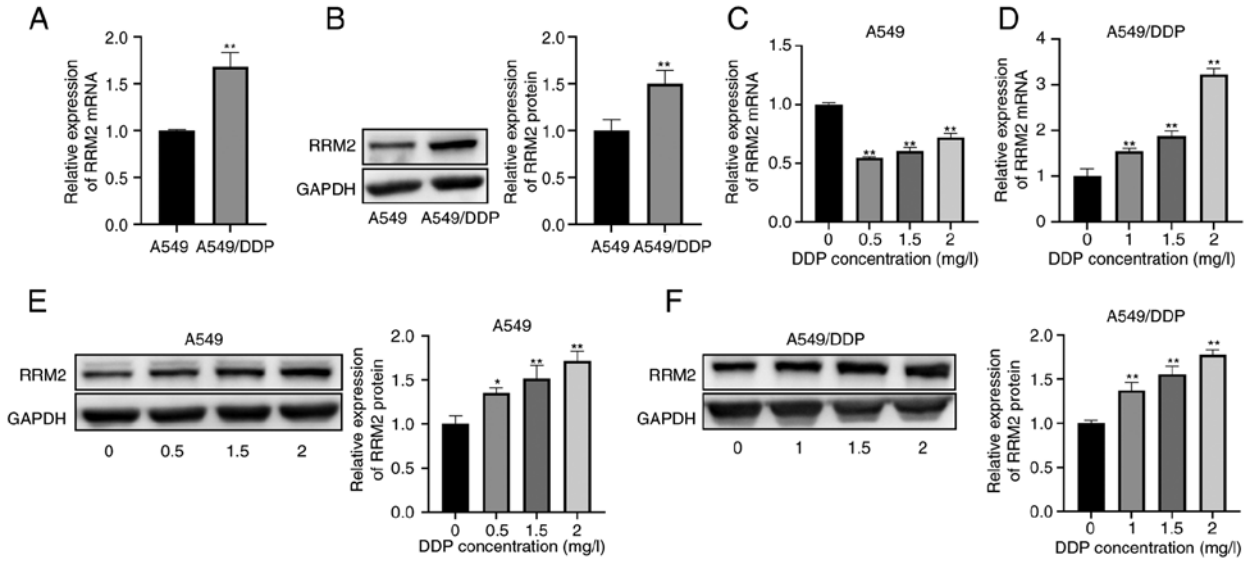

Figure 3. Induction of RRM2 expression by cisplatin in lung adenocarcinoma cell lines. (A) RT-qPCR and (B) western blot analysis of RRM2 expression in A549 and A549/DDP cells. RRM2 expression in A549 and A549/DDP cells treated with different concentrations of cisplatin for 48 h. RRM2 expression in (C) A549 and (D) A549/DDP cells by RT-qPCR and (E) A549 and (F) A549/DDP cells by western blot analysis. *P<0.05, **P<0.01 vs. A549 or 0 groups. RRM2, ribonucleotide reductase M2; A549/DDP, A549 cells with cisplatin resistance; RT-qPCR, reverse transcription-quantitative PCR.

that correlated with the concentration of cisplatin used, both at the mRNA and protein levels (Fig. 3D and F).

RRM2 knockdown reduces lung adenocarcinoma cell proliferation and migration, promotes apoptosis and partially restores their sensitivity to cisplatin. To investigate the role of RRM2 in lung adenocarcinoma cells, lentivirus was used to knock down RRM2 in lung adenocarcinoma cells (Fig. 4A and B). The results indicated that RRM2 knockdown inhibited the proliferation (Fig. 4C and F) and migration (Fig. 4E) of A549 and A549/DDP cells, and also increased the number of cells arrested in the S phase of the cell cycle (Fig. 4D). The CCK-8 toxicity assay showed that RRM2 knockdown resulted in increased inhibition of cell growth by cisplatin (Fig. 4G). In addition, flow cytometry experiments indicated that RRM2 knockdown not only increased apoptosis in A549 and A549/DDP cells, but also enhanced the effect of cisplatin on these cells (Fig. 4H). Importantly, during the apoptosis experiments, different concentrations of DDP were used for treating the native A549 cell line and the DDP-resistant cell line. Specifically, the native A549 cell line was treated with DDP at a concentration of 2 μg/ml, whereas the DDP-resistant cell line was exposed to DDP at a concentration of 8 μg/ml. This discrepancy in DDP concentrations contributed to the higher apoptosis rate observed in the DDP-resistant cell line compared to the native A549 cell line in the NC + DDP group (Fig. 4H).

RRM2 promotes the development of lung adenocarcinoma through the Wnt/β-catenin signaling pathway. Camptothecin facilitates the translocation of RRM2 into the nucleus. Knockdown of RRM2 enhances the effect of camptothecin on DNA damage in the cell (24). To investigate the precise mechanism of action of RRM2 in lung adenocarcinoma, A549 and A549/DDP cells were treated with or without 2 μg/ml cisplatin for 24 h, and they were examined by laser confocal microscopy. The results suggested that cisplatin treatment did not induce nuclear translocation of RRM2 in either A549 or A549/DDP cells (Fig. 5A). Therefore, it was postulated that the influence of RRM2 in promoting cellular resistance to cisplatin was not exerted through nuclear translocation. Subsequently, it was found that the expression levels of β-catenin, c-Myc and cyclin D1 were reduced in A549 and A549/DDP cells after RRM2 knockdown, as demonstrated by western blot analysis (Fig. 5B). In conclusion, knockdown of RRM2 had an inhibitory effect on lung adenocarcinoma via the Wnt/β-catenin signaling pathway.

β-Catenin overexpression partially reverses the effect of RRM2 knockdown on lung adenocarcinoma cells. In a rescue experiment, pcDNA was used to overexpress β-catenin in A549 cells with RRM2 knockdown (Fig. 6A and B). Through western blot analysis of proteins involved in the Wnt/β-catenin signaling pathway, it was found that β-catenin overexpression restored the expression of c-Myc and cyclin D1 in A549 cells (Fig. 6B). β-Catenin overexpression not only accelerated the proliferation (Fig. 6C and D) and migration (Fig. 6F) of A549 cells, but it also reduced the number of cells originally blocked in the S phase (Fig. 6E). In CCK-8 toxicity assays, β-catenin overexpression attenuated the inhibitory effect of cisplatin on cells (Fig. 6G). Furthermore, flow cytometry demonstrated that treatment of A549 cells overexpressing β-catenin with or without 2 μg/ml of cisplatin resulted in the finding that overexpression of β-catenin reduced the effect of RRM2 knockdown on A549 cells (Fig. 6H).

Discussion

Cancer cells are known for their ability to grow uncontrollably, which may lead to damage to surrounding tissues and impaired organ function. In addition, cancer cells with abnormal expression of MMP2, MMP9, N-cadherin, E-cadherin and other

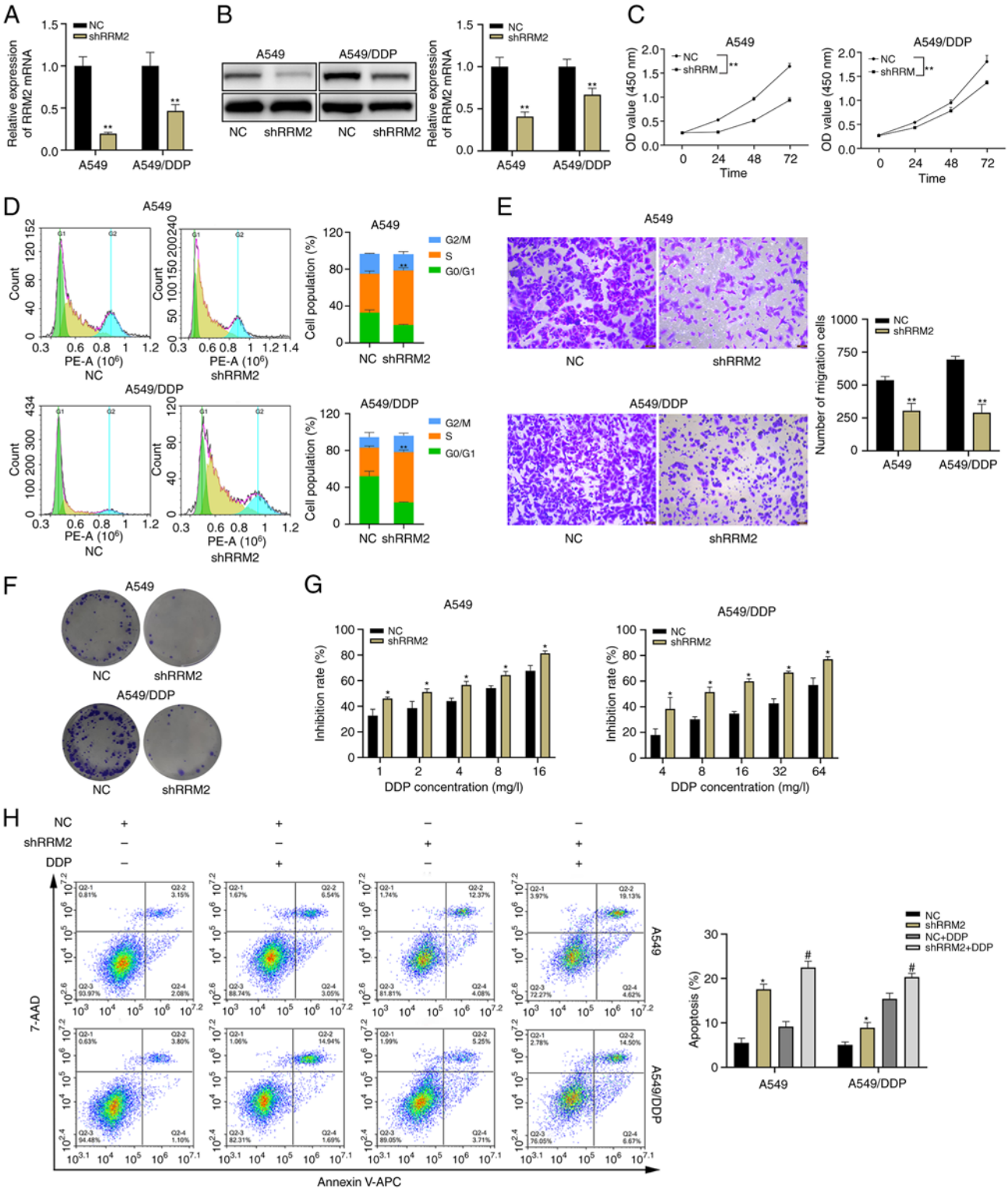

Figure 4. Effect of RRM2 knockdown on lung adenocarcinoma cells with and without cisplatin resistance. (A) Reverse transcription-quantitative PCR and (B) western blot analysis confirmed the efficacy of RRM2 knockdown. (C) RRM2 knockdown suppressed cell proliferation. (D) RRM2 knockdown caused cell cycle arrest in the S-phase. (E) Transwell assays indicated that RRM2 knockdown inhibited cell migration (magnification, x200). (F) In the colony-formation assay, RRM2 knockdown had an inhibitory effect. (G) RRM2 knockdown partially restored cisplatin sensitivity in the cells. (H) RRM2 knockdown promoted apoptosis and enhanced cisplatin-induced cytotoxicity in the cells. *P<0.05, **P<0.01 vs. NC; $^{\#}$P<0.05 vs. NC+DDP. RRM2, ribonucleotide reductase M2; NC, negative control; A549/DDP, A549 cells with cisplatin resistance; shRRM2, short hairpin RNA targeting RRM2; OD, optical density.

proteins are more likely to metastasize by breaking through the basement membrane (25,26). Cisplatin is a widely used chemotherapeutic drug for the treatment of advanced tumors, as it works by forming DNA cross-links in cancer cells, which leads to inhibition of DNA replication and transcription, ultimately causing cell cycle arrest and apoptosis (27). However, in cancer cells, DNA damage repair processes, such as nucleotide excision repair, post-replication repair and homologous

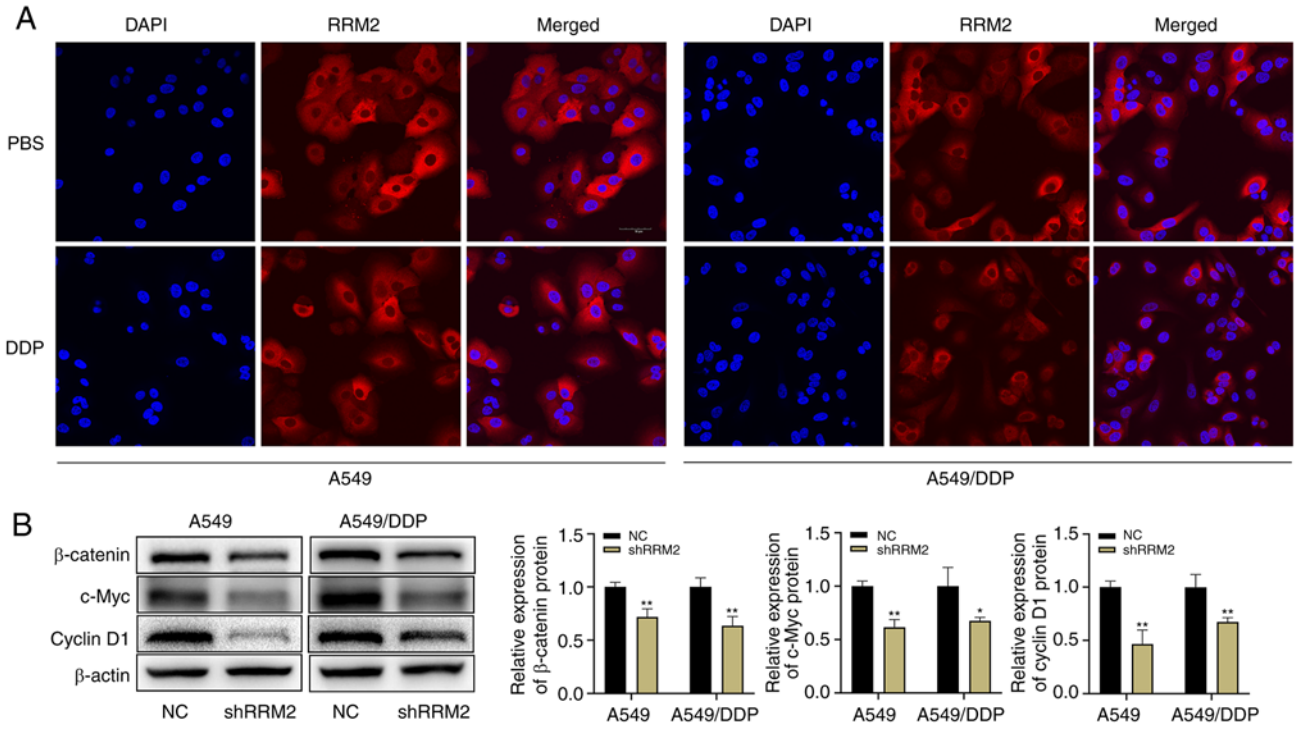

Figure 5. Mechanism of RRM2 action in lung adenocarcinoma. (A) Cellular localization of RRM2 (scale bar, 50 μm). (B) Expression levels of related proteins in the Wnt/β-catenin signaling pathway after knockdown of RRM2. *P<0.05, **P<0.01. RRM2, ribonucleotide reductase M2; NC, negative control; A549/DDP, A549 cells with cisplatin resistance; shRRM2, short hairpin RNA targeting RRM2.

recombination repair, may counteract the effects of cisplatin, resulting in cisplatin resistance (28). Recent studies have indicated that RRM2, an oncogene, plays a critical role in the proliferation, migration, invasion, and drug resistance of breast cancer cells, small cell lung cancer cells, renal clear cell carcinoma cells, and pancreatic cancer cells (29-32). In lung adenocarcinoma, suppression of RRM2 also inhibits the proliferation, migration and invasive ability of lung adenocarcinoma cells (33-36). However, there is still limited research on the specific mechanism of action of RRM2 in lung adenocarcinoma. The present study aimed to investigate RRM2 expression, immune infiltration and its mechanism of action in lung adenocarcinoma.

In the present study, a bioinformatics analysis was conducted, which found that RRM2 was highly expressed in lung adenocarcinoma, and there was an association of RRM2 with tumor size and metastasis. Patients with high RRM2 expression in lung adenocarcinoma had poor prognosis, and RRM2 was indicated to hold significant predictive value for the 5-year survival of patients. The results of enrichment analyses suggested that the mechanism of action of RRM2 in lung adenocarcinoma may involve cell cycle regulation. TME analysis showed that patients with high RRM2 expression had fewer stromal cells and lower tumor purity, which may contribute to their poor prognosis. However, the ImmuneScore did not significantly differ between patients with varying levels of RRM2. In the present study, differential and correlation analyses of several types of immune cell in the tumor tissue of patients with lung adenocarcinoma were performed and it was indicated that the levels of 12 immune cells differed between patients expressing different levels of RRM2. Furthermore, six immune cell types exhibited a positive correlation with RRM2 expression levels, while seven immune cell types showed a negative correlation with RRM2 expression levels. In cellular experiments, the expression of RRM2 was found to be higher in cisplatin-resistant A549 cells than in A549 cells. The expression level of RRM2 in the cells increased with increasing cisplatin concentration. However, a noteworthy phenomenon emerged: Although cisplatin induced protein expression of RRM2, the mRNA expression level of RRM2 decreased in cisplatin-treated A549 cells compared to that in untreated A549 cells. This decrease in RRM2 mRNA expression in cisplatin-treated A549 cells is likely due to the inhibitory effect of cisplatin on tumor cell DNA replication and transcription by causing DNA cross-linking in tumor cells. However, other mechanisms appear to affect RRM2 mRNA translation and post-translational modifications, resulting in no decrease in RRM2 protein expression. It may be suggested that RRM2 has a role in the development of lung adenocarcinoma and is associated with the development of cisplatin resistance.

Based on the results of the previous analyses, the present study aimed to investigate the specific mechanisms of action of RRM2 in the cell cycle and cisplatin resistance of lung adenocarcinoma. Lentivirus was used to stably knock down RRM2 in A549 and A549/DDP cells and it was found that knockdown of RRM2 slowed down cell proliferation and migration, increased their sensitivity to cisplatin and promoted apoptosis. These findings align with the discoveries made by Liu *et al* (33). Furthermore, the present study demonstrated, through cell cycle experiments, that the depletion of RRM2 in lung adenocarcinoma cells led to an increased population of cells with cell cycle arrest in S phase. This phenomenon may potentially account for the observed inhibition of cancer

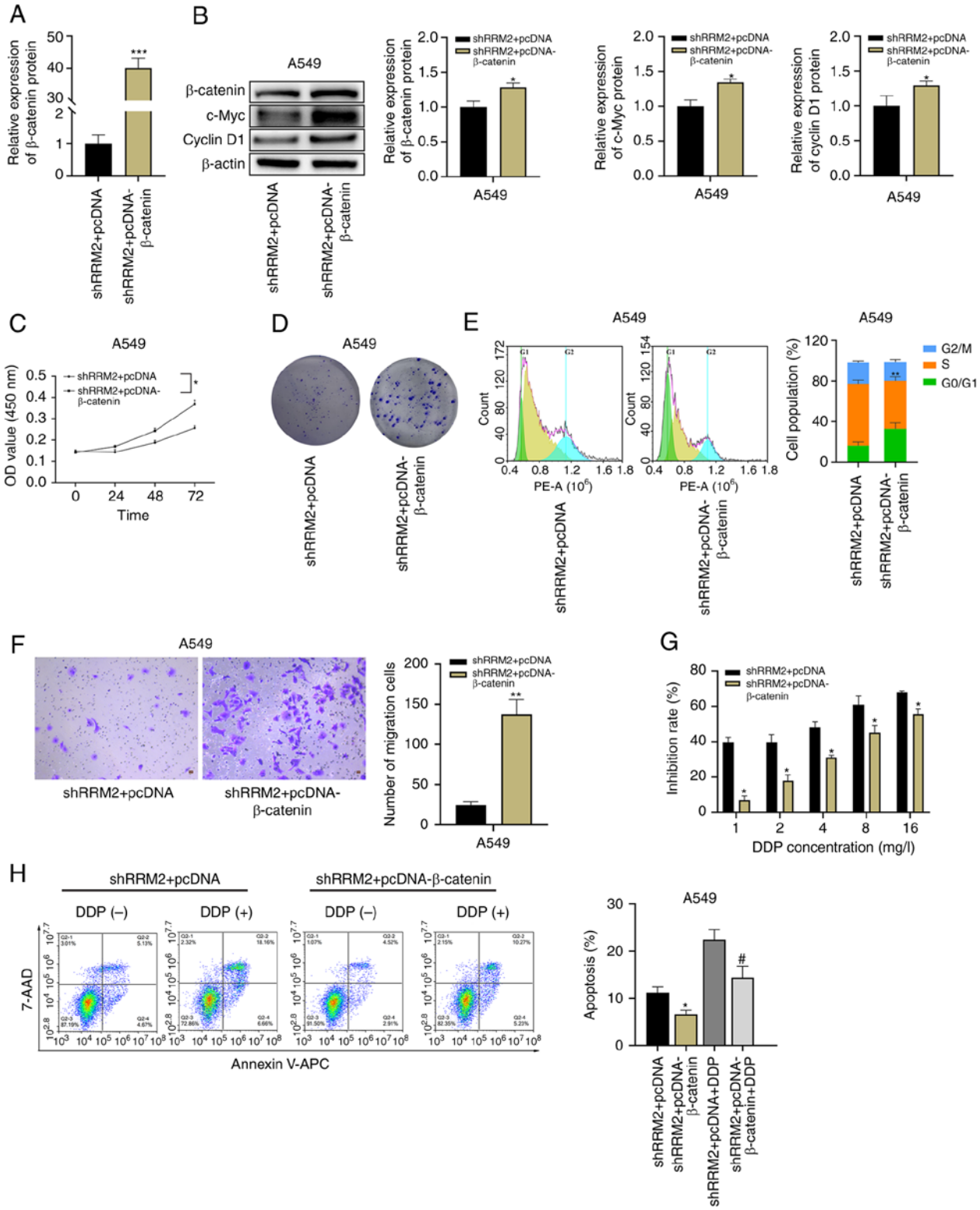

Figure 6. Partial reversal of RRM2 knockdown effect by β-catenin overexpression in lung adenocarcinoma cells. (A) Detection of β-catenin expression levels using reverse transcription-quantitative PCR. (B) Expression levels of related proteins in the Wnt/β-catenin signaling pathway after β-catenin overexpression in cells with simultaneous RRM2 knockdown. Promotion of (C) cell proliferation and (D) colony formation by β-catenin overexpression in cells with simultaneous RRM2 knockdown. (E) Reduction of cells blocked in S-phase after β-catenin overexpression. (F) Promotion of cell migration by β-catenin overexpression in cells with simultaneous RRM2 knockdown (magnification, x200x). (G) Attenuation of cell sensitivity to cisplatin by β-catenin overexpression in cells with simultaneous RRM2 knockdown. (H) Inhibition of apoptosis by β-catenin overexpression in cells with simultaneous RRM2 knockdown, reducing the cytotoxic effect of cisplatin on the cells. *P<0.05, **P<0.01, ***P<0.001 vs. NC; $^{\#}$P<0.05 vs. NC + DDP. RRM2, ribonucleotide reductase M2; shRRM2, short hairpin RNA targeting RRM2; NC, negative control; OD, optical density.

cell proliferation, restoration of cisplatin sensitivity in lung adenocarcinoma cells and facilitation of apoptosis. The cell cycle analysis results suggested that RRM2 knockdown inhibited cell proliferation and activated programmed cell death by

blocking the cell cycle in S phase. Previous studies suggested that RRM2 may be involved in cancer development by regulating the activation of the Wnt/β-catenin signaling pathway. In the present study, the expression of related proteins in this pathway was examined and it was found that the expression levels of β-catenin, c-Myc and cyclin D1 were decreased after RRM2 knockdown. This suggests that RRM2 may be involved in the regulation of the Wnt/β-catenin signaling pathway in lung adenocarcinoma. To further clarify the relationship between RRM2 and the Wnt/β-catenin signaling pathway, β-catenin was overexpressed using pcDNA3.1 in cells with knockdown RRM2. The results showed that overexpression of β-catenin attenuated the effect of RRM2 knockdown on A549 cells. However, despite attempts to overexpress β-catenin in A549/DDP cells, successful transfection could only be achieved in A549 cells. Therefore, only A549 cells were used for the subsequent overexpression experiments. In addition, only one cell line, A549, and its cisplatin-resistant variant, A549/DDP, was used for experimental validation throughout the study. This is one of the limitations of the present study, as the use of a single cell line does not eliminate the influence of a single genetic background on the obtained results.

Regarding the downstream mechanisms of RRM2 in lung adenocarcinoma, Ma *et al* (34) discovered that RRM2 may influence the sensitivity of A549 cells to gemcitabine by modulating the phosphorylated phosphatase and tensin homolog/PI3K/AKT signaling pathway. Another study demonstrated that suppression of RRM2 expression not only inhibits the malignant behavior of lung adenocarcinoma cells but also synergistically enhances the efficacy of radiotherapy in inducing cell death (35). This synergistic effect is achieved through the activation of the GMP-AMP synthase/stimulator of interferon genes signaling pathway. A separate study by Cao *et al* (36) showed that RRM2 may be regulated by microRNA-202-3p. Downregulation of RRM2 results in inhibited proliferation, migration and invasion of lung adenocarcinoma cells, possibly through the Notch signaling pathway. However, Cao *et al* (36) solely employed KEGG enrichment analysis to suggest the involvement of the Notch signaling pathway in the RRM2-mediated effects on lung adenocarcinoma, without conducting experimental validation.

In conclusion, the present study demonstrated that RRM2 is highly expressed in lung adenocarcinoma tissues and that its expression is higher in cisplatin-resistant lung adenocarcinoma cells compared to non-cisplatin-resistant cells. Cisplatin also induces RRM2 expression in a dose-dependent manner. Knockdown of RRM2 inhibited the malignant behavior of lung adenocarcinoma cells. On the other hand, overexpression of β-catenin attenuated the effects of RRM2 knockdown, suggesting that RRM2 may affect lung adenocarcinoma development through the Wnt/β-catenin signaling pathway. The present study provided further insight into the mechanism of RRM2 action in lung adenocarcinoma and suggests that RRM2 may be a promising therapeutic target for the treatment of this disease.

Acknowledgements

Not applicable.

Funding

No funding was received.

Availability of data and materials

The datasets used and/or analyzed during the current study are available from the corresponding author on reasonable request.

Authors' contributions

YJ, XH and LJ designed the study, performed the experiments and wrote the manuscript. BR, YH and MP performed the statistical analysis. BR and LH collected the mRNA transcriptome data from public databases and conducted the data analysis. LH and LJ critically revised the manuscript and confirmed the authenticity of the data before submission. All authors have read and approved the final version of the manuscript.

Ethics approval and consent to participate

Not applicable.

Patient consent for publication

Not applicable.

Competing interests

The authors declare that they have no competing interests.

References

1. Sung H, Ferlay J, Siegel RL, Laversanne M, Soerjomataram I, Jemal A and Bray F: Global cancer statistics 2020: GLOBOCAN estimates of incidence and mortality worldwide for 36 cancers in 185 countries. CA Cancer J Clin 71: 209-249, 2021.
2. Liu X, Liu B, Li R, Wang F, Wang N, Zhang M, Bai Y, Wu J, Liu L, Han D, *et al*: miR-146a-5p plays an oncogenic role in NSCLC via suppression of TRAF6. Front Cell Dev Biol 8: 847, 2020.
3. Hellmann MD, Li BT, Chaft JE and Kris MG: Chemotherapy remains an essential element of personalized care for persons with lung cancers. Ann Oncol 27: 1829-1835, 2016.
4. Sarin N, Engel F, Kalayda GV, Mannewitz M, Cinatl J Jr, Rothweiler F, Michaelis M, Saafan H, Ritter CA, Jaehde U and Frötschl R: Cisplatin resistance in non-small cell lung cancer cells is associated with an abrogation of cisplatin-induced G2/M cell cycle arrest. PLoS One 12: e181081, 2017.
5. Mazzu YZ, Armenia J, Chakraborty G, Yoshikawa Y, Coggins SA, Nandakumar S, Gerke TA, Pomerantz MM, Qiu X, Zhao H, *et al*: A novel mechanism driving poor-prognosis prostate cancer: Overexpression of the DNA repair gene, ribonucleotide reductase small subunit M2 (RRM2). Clin Cancer Res 25: 4480-4492, 2019.
6. Duxbury MS, Ito H, Zinner MJ, Ashley SW and Whang EE: RNA interference targeting the M2 subunit of ribonucleotide reductase enhances pancreatic adenocarcinoma chemosensitivity to gemcitabine. Oncogene 23: 1539-1548, 2004.
7. Peng S, Yi L, Liao L, Bin Y, Qu W and Hu H: Circ_0008285 knockdown represses tumor development by miR-384/RRM2 axis in hepatocellular carcinoma. Ann Hepatol 27: 100743, 2022.
8. Liu Q, Guo L, Qi H, Lou M, Wang R, Hai B, Xu K, Zhu L, Ding Y, Li C, *et al*: A MYBL2 complex for RRM2 transactivation and the synthetic effect of MYBL2 knockdown with WEE1 inhibition against colorectal cancer. Cell Death Dis 12: 683, 2021.
9. Chang CC, Lin CC, Wang CH, Huang CC, Ke TW, Wei PL, Yeh KT, Hsu KC, Hsu NY and Cheng YW: MiR-211 regulates the expression of RRM2 in tumoral metastasis and recurrence in colorectal cancer patients with a k-ras gene mutation. Oncol Lett 15: 8107-8117, 2018.

10. Liu Q, Song C, Li J, Liu M, Fu L, Jiang J, Zeng Z and Zhu H: E2F2 enhances the chemoresistance of pancreatic cancer to gemcitabine by regulating the cell cycle and upregulating the expression of RRM2. Med Oncol 39: 124, 2022.
11. Lu H, Lu S, Yang D, Zhang L, Ye J, Li M and Hu W: MiR-20a-5p regulates gemcitabine chemosensitivity by targeting RRM2 in pancreatic cancer cells and serves as a predictor for gemcitabine-based chemotherapy. Biosci Rep 39: BSR20181374, 2019.
12. Chen P, Wu JN, Shu Y, Jiang HG, Zhao XH, Qian H, Chen K, Lan T, Chen CG and Li J: Gemcitabine resistance mediated by ribonucleotide reductase M2 in lung squamous cell carcinoma is reversed by GW8510 through autophagy induction. Clin Sci (Lond) 132: 1417-1433, 2018.
13. Chen CW, Li Y, Hu S, Zhou W, Meng Y, Li Z, Zhang Y, Sun J, Bo Z, DePamphilis ML, *et al*: DHS (trans-4,4'-dihydroxystilbene) suppresses DNA replication and tumor growth by inhibiting RRM2 (ribonucleotide reductase regulatory subunit M2). Oncogene 38: 2364-2379, 2019.
14. Xue T, Wang L, Li Y, Song H, Chu H, Yang H, Guo A and Jiao J: SiRNA-mediated RRM2 gene silencing combined with cisplatin in the treatment of epithelial ovarian cancer in vivo: An experimental study of nude mice. Int J Med Sci 16: 1510-1516, 2019.
15. Zhang M, Wang J, Yao R and Wang L: Small interfering RNA (siRNA)-mediated silencing of the M2 subunit of ribonucleotide reductase: A novel therapeutic strategy in ovarian cancer. Int J Gynecol Cancer 23: 659-666, 2013.
16. Wang L, Meng L, Wang XW, Ma GY and Chen JH: Expression of RRM1 and RRM2 as a novel prognostic marker in advanced non-small cell lung cancer receiving chemotherapy. Tumour Biol 35: 1899-1906, 2014.
17. Deng Y, Chen X, Huang C, Song J, Feng S, Chen X and Zhou R: Screening and validation of significant genes with poor prognosis in pathologic stage-I lung adenocarcinoma. J Oncol 2022: 3794021, 2022.
18. Grossi F, Dal Bello MG, Salvi S, Puzone R, Pfeffer U, Fontana V, Alama A, Rijavec E, Barletta G, Genova C, *et al*: Expression of ribonucleotide reductase subunit-2 and thymidylate synthase correlates with poor prognosis in patients with resected stages I-III non-small cell lung cancer. Dis Markers 2015: 302649, 2015.
19. DasGupta R, Kaykas A, Moon RT and Perrimon N: Functional genomic analysis of the Wnt-wingless signaling pathway. Science 308: 826-833, 2005.
20. Brown AM: Canonical Wnt signaling: High-throughput RNAi widens the path. Genome Biol 6: 231, 2005.
21. Xu H and Li B: MicroRNA-582-3p targeting ribonucleotide reductase regulatory subunit M2 inhibits the tumorigenesis of hepatocellular carcinoma by regulating the Wnt/β-catenin signaling pathway. Bioengineered 13: 12876-12887, 2022.
22. Liu X, Peng J, Zhou Y, Xie B and Wang J: Silencing RRM2 inhibits multiple myeloma by targeting the Wnt/beta-catenin signaling pathway. Mol Med Rep 20: 2159-2166, 2019.
23. Livak KJ and Schmittgen TD: Analysis of relative gene expression data using real-time quantitative PCR and the 2(-Delta Delta C(T)) method. Methods 25: 402-408, 2001.
24. Zhang YW, Jones TL, Martin SE, Caplen NJ and Pommier Y: Implication of checkpoint kinase-dependent up-regulation of ribonucleotide reductase R2 in DNA damage response. J Biol Chem 284: 18085-18095, 2009.
25. Cabral-Pacheco GA, Garza-Veloz I, Castruita-De LRC, Ramirez-Acuna JM, Perez-Romero BA, Guerrero-Rodriguez JF, Martinez-Avila N and Martinez-Fierro ML: The roles of matrix metalloproteinases and their inhibitors in human diseases. Int J Mol Sci 21: 9739, 2020.
26. Sisto M, Ribatti D and Lisi S: Cadherin signaling in cancer and autoimmune diseases. Int J Mol Sci 22: 13358, 2021.
27. Dasari S and Tchounwou PB: Cisplatin in cancer therapy: Molecular mechanisms of action. Eur J Pharmacol 740: 364-378, 2014.
28. Kryczka J, Kryczka J, Czarnecka-Chrebelska KH and Brzezianska-Lasota E: Molecular mechanisms of chemoresistance induced by cisplatin in NSCLC cancer therapy. Int J Mol Sci 22: 8885, 2021.
29. Li S, Mai H, Zhu Y, Li G, Sun J, Li G, Liang B and Chen S: MicroRNA-4500 inhibits migration, invasion, and angiogenesis of breast cancer cells via RRM2-dependent MAPK signaling pathway. Mol Ther Nucleic Acids 21: 278-289, 2020.
30. Khan P, Siddiqui JA, Kshirsagar PG, Venkata RC, Maurya SK, Mirzapoiazova T, Perumal N, Chaudhary S, Kanchan RK, Fatima M, *et al*: MicroRNA-1 attenuates the growth and metastasis of small cell lung cancer through CXCR4/FOXM1/RRM2 axis. Mol Cancer 22: 1, 2023.
31. Zou Y, Zhou J, Xu B, Li W and Wang Z: Ribonucleotide reductase subunit M2 as a novel target for clear-cell renal cell carcinoma. Onco Targets Ther 12: 3267-3275, 2019.
32. Shan J, Wang Z, Mo Q, Long J, Fan Y, Cheng L, Zhang T, Liu X and Wang X: Ribonucleotide reductase M2 subunit silencing suppresses tumorigenesis in pancreatic cancer via inactivation of PI3K/AKT/mTOR pathway. Pancreatology 22: 401-413, 2022.
33. Liu Y, Zhang Y, Li Q, Xu R and Huang N: MiR-200c-3p and miR-485-5p overexpression elevates cisplatin sensitivity and suppresses the malignant phenotypes of non-small cell lung cancer cells through targeting RRM2. Thorac Cancer 13: 1974-1985, 2022.
34. Ma X, Fu T, Ke ZY, Du SL, Wang XC, Zhou N, Zhong MY, Liu YJ and Liang AL: MiR-17- 5p/RRM2 regulated gemcitabine resistance in lung cancer A549 cells. Cell Cycle 22: 1367-1379, 2023.
35. Jiang X, Li Y, Zhang N, Gao Y, Han L, Li S, Li J, Liu X, Gong Y and Xie C: RRM2 silencing suppresses malignant phenotype and enhances radiosensitivity via activating cGAS/STING signaling pathway in lung adenocarcinoma. Cell Biosci 11: 74, 2021.
36. Cao X, Xue F, Chen H, Shen L, Yuan X, Yu Y, Zong Y, Zhong L and Huang F: MiR-202-3p inhibits the proliferation and metastasis of lung adenocarcinoma cells by targeting RRM2. Ann Transl Med 10: 1374, 2022.